

# Measurement of the Flux of Ultrahigh Energy Cosmic Rays from Monocular Observations by the High Resolution Fly's Eye Experiment.

T. Abu-Zayyad,<sup>1</sup> J.F. Amann,<sup>2</sup> G. Archbold,<sup>1</sup> J.A. Bellido,<sup>3</sup> K. Belov,<sup>1</sup> J.W. Belz,<sup>4</sup> D.R. Bergman,<sup>5</sup> Z. Cao,<sup>1</sup> R.W. Clay,<sup>3</sup> M.D. Cooper,<sup>2</sup> H. Dai,<sup>1</sup> B.R. Dawson,<sup>3</sup> A.A. Everett,<sup>1</sup> J.H.V. Girard,<sup>1</sup> R.C. Gray,<sup>1</sup> W.F. Hanlon,<sup>1</sup> C.M. Hoffman,<sup>2</sup> M.H. Holzschneider,<sup>2</sup> P. Hüntemeyer,<sup>1</sup> B.F. Jones,<sup>1</sup> C.C.H. Jui,<sup>1</sup> D.B. Kieda,<sup>1</sup> K. Kim,<sup>1</sup> E.C. Loh,<sup>1</sup> N. Manago,<sup>6</sup> L.J. Marek,<sup>2</sup> K. Martens,<sup>1</sup> G. Martin,<sup>7</sup> J.A.J. Matthews,<sup>7</sup> J.N. Matthews,<sup>1</sup> S. Meltzer,<sup>8</sup> J.R. Meyer,<sup>1</sup> S.A. Moore,<sup>1</sup> P. Morrison,<sup>1</sup> A.N. Moosman,<sup>1</sup> J.R. Mumford,<sup>1</sup> M.W. Munro,<sup>4</sup> C.A. Painter,<sup>2</sup> L. Perera,<sup>5</sup> K. Reil,<sup>1</sup> R. Riehle,<sup>1</sup> M. Roberts,<sup>7</sup> J.S. Sarracino,<sup>2</sup> M. Sasaki,<sup>6</sup> M.A. Schindler,<sup>4</sup> S.R. Schnetzer,<sup>5</sup> P. Shen,<sup>1</sup> K.M. Simpson,<sup>3</sup> G. Sinnis,<sup>2</sup> J.D. Smith,<sup>1</sup> P. Sokolsky,<sup>1</sup> C. Song,<sup>8</sup> R.W. Springer,<sup>1</sup> B.T. Stokes,<sup>1</sup> S.F. Taylor,<sup>1</sup> S.B. Thomas,<sup>1</sup> T.N. Thompson,<sup>2</sup> G.B. Thomson,<sup>5</sup> D. Tupa,<sup>2</sup> S. Westerhoff,<sup>8</sup> L.R. Wiencke,<sup>1</sup> T.D. VanderVeen,<sup>1</sup> A. Zech,<sup>5</sup> and X. Zhang<sup>8</sup>

(The High Resolution Fly's Eye Collaboration)

<sup>1</sup>*University of Utah, Department of Physics and High Energy Astrophysics Institute, Salt Lake City, Utah, USA*

<sup>2</sup>*Los Alamos National Laboratory, Los Alamos, NM, USA*

<sup>3</sup>*University of Adelaide, Department of Physics, Adelaide, South Australia, Australia*

<sup>4</sup>*University of Montana, Department of Physics and Astronomy, Missoula, Montana, USA.*

<sup>5</sup>*Rutgers — The State University of New Jersey,*

*Department of Physics and Astronomy, Piscataway, New Jersey, USA*

<sup>6</sup>*University of Tokyo, Institute for Cosmic Ray Research, Kashiwa, Japan*

<sup>7</sup>*University of New Mexico, Department of Physics and Astronomy, Albuquerque, New Mexico, USA*

<sup>8</sup>*Columbia University, Department of Physics and Nevis Laboratory, New York, New York, USA*

We have measured the cosmic ray spectrum above  $10^{17}$  eV using the two air fluorescence detectors of the High Resolution Fly's Eye observatory operating in monocular mode. We describe the detector, photo-tube and atmospheric calibrations, as well as the analysis techniques for the two detectors. We fit the spectrum to a model consisting of galactic and extra-galactic sources. The measured spectrum is consistent with this two-component model including the GZK cutoff.

The highest energy cosmic rays detected so far, of energies up to and exceeding  $10^{20}$  eV, are very interesting in that they shed light on two important questions: the nature of their origin in astrophysical or other sources and their propagation to us through the Cosmic Microwave Background Radiation (CMBR). The production of pions from interactions of CMBR photons and ultra high energy cosmic rays (UHECR) is an important energy loss mechanism above  $\sim 6 \times 10^{19}$  eV, and produces the Greisen-Zatsepin-K'uzmin (GZK) cut-off [1, 2];  $e^+e^-$  production in the same collisions is a weaker energy-loss mechanism above a threshold of  $\sim 7 \times 10^{17}$  eV. We report here the flux of UHECR from  $2 \times 10^{17}$  eV to over  $10^{20}$  eV, measured in monocular mode, with the High Resolution Fly's Eye (HiRes) detectors.

The HiRes observatory consists of two air-fluorescence detector sites separated by 12.6 km and located at the U.S. Army Dugway Proving Ground in Utah. Cosmic rays interacting in the upper atmosphere initiate particle cascades known as extensive air-showers. Passage of charged particles excites nitrogen molecules causing emission of (mostly) ultraviolet light. The fluorescence yield per particle has been previously measured [3]. From the observed signal and its longitudinal development, we can infer the arrival direction, energy, and composition of the primary cosmic ray. HiRes was designed to detect this fluorescence light stereoscopically. However our two de-

tectors trigger and reconstruct events independently, and in this "monocular" mode our current data have the best statistical power and cover the widest energy range.

The two HiRes detector sites, referred to as HiRes-I and HiRes-II, are operated on clear, moon-less nights. Over a typical year, each detector accumulates up to 1000 hours of observation. The HiRes-I site has been in operation since June of 1997 [4]. It consists of 22 detector units, each equipped with a 5 m<sup>2</sup> spherical mirror and 256 photo-tube pixels at its focal plane. Each photo-tube covers a 1° cone of sky. These 22 mirrors cover elevation angles between 3° and 17°. The HiRes-I detectors perform sample-and-hold integration in a 5.6  $\mu$ s window, which is long enough to contain signals from all reconstructible events. The HiRes-II site was completed in late 1999 and began observations that year. This site uses the same type of mirrors and photo-tubes as HiRes-I, but contains 42 mirrors, in two rings, covering elevation angles from 3° to 31°. HiRes-II uses an FADC data acquisition system operating at 10 MHz [5]. Both the HiRes-I and -II sites provide  $2\pi$  azimuthal angle coverage.

To determine the correct shower energies, the air fluorescence technique requires accurate measurement and monitoring of photo-tube gains. Two methods of calibration are used. Pulses from a YAG laser are distributed to mirrors via optical fibers. They provide a nightly relative calibration. A stable, standard light source is used for a

more precise monthly absolute calibration. Overall, the relative photo-tube gains were stable to within 3.5% and the absolute gains were known to  $\pm 10\%$  [6].

A second variable in the energy measurement is atmospheric clarity. Light from air showers is attenuated by: (a) molecular (Rayleigh), and (b) aerosol scattering. The former is approximately constant, subject only to small variations in the atmospheric overburden. The aerosol concentration varies with time. HiRes measures the aerosol content by observing scattered light from two steerable laser systems. The laser observed by HiRes-I has been in operation since 1999. The vertical aerosol optical depth from ground to 3.5 km altitude,  $\tau_A$ , is measured each hour (the vertical transmission through the aerosol is  $T = \exp -\tau_A$ ). These measurements yielded an average  $\tau_A$  at 355 nm of 0.04 [7]. The RMS of the distribution is 0.02, and the systematic uncertainty in the mean is less than this. The average aerosol ground-level horizontal extinction length,  $\Lambda_H$ , was determined to be 25 km. Because much of our data were collected before the steerable lasers were in operation we used these averages in our analysis and simulation programs.

Between June 1997 and February 2003, the HiRes-I detector operated for approximately 3600 hours. From this, 2820 hours of good weather data were selected. This data set contained 145 million triggers, mostly noise events. A subset of 5.5 million downward track-like events were found. For these events, a shower-detector plane was determined from the pattern of photo-tube hits. We then excluded events containing an average number of photo-electrons per photo-tube of less than 25; for these the fluctuations in signals are too great to permit reliable reconstruction of the shower profile. Lastly, we cut out tracks with angular speed in excess of  $3.33^\circ/\mu\text{s}$ , which are typically within 5 km of HiRes-I. For these events, the shower maxima appear above the field of view. We selected 12,709 events for reconstruction.

Determination of the shower geometry is possible using a single detector (i.e. in monocular mode). The plane containing the air shower and the detector is found from the pattern of hits. The impact parameter,  $R_p$ , and the in-plane angle between the shower and the horizontal plane containing the detector,  $\psi$ , are determined by fitting the photo-tube trigger times,  $t_i$ , to the following function of their viewing angles,  $\chi_i$ , measured in the event plane from the horizontal [8]:

$$t_i = t_0 + \frac{R_p}{c} \tan \left( \frac{\pi - \psi - \chi_i}{2} \right). \quad (1)$$

Here  $t_0$  is the time of closest approach. However, with limited elevation coverage, HiRes-I monocular events are too short in angular spread for reliable determination of  $\psi$  and  $R_p$  by timing alone. For this analysis, the expected form of the shower development itself was used to constrain the time fit to yield realistic geometries. The

shower profile is assumed to be described by the Gaisser-Hillas parameterization [9].

$$N(x) = N_m \left( \frac{x - x_0}{x_m - x_0} \right)^{(x_m - x_0)/\lambda} \exp \left( -\frac{x_m - x}{\lambda} \right), \quad (2)$$

where  $N(x)$ ,  $N_m$  are the number of particles at depth  $x$  and at shower maximum depth,  $x_m$ , and  $x_0$  and  $\lambda$  are shower shape parameters. Equation 2 is in good agreement with previous HiRes measurements [10] and with CORSIKA/QGSJET simulations [11, 12, 13]. This technique is called the Profile-Constrained Fit (PCF). We allowed  $x_m$  to vary in  $35 \text{ g/cm}^2$  steps between 680 and  $900 \text{ g/cm}^2$ , matching the expected range of  $x_m$  for proton to iron primaries in this energy range. Next, we require a minimum track arc length of  $8.0^\circ$  and a maximum depth for the highest elevation hit of  $1000 \text{ g/cm}^2$ . Significant contamination from direct Čerenkov light degrades the reliability of the PCF. Therefore, we also rejected tracks with  $\psi > 120^\circ$  and those with two or more bins with  $> 25\%$  Čerenkov light. A total of 6,920 events remained.

Monte Carlo studies were performed to assess the reliability of the PCF method. The simulated events were subjected to the same selection criteria and cuts imposed on the data. Not including atmospheric fluctuations, an RMS energy resolution of better than 20% was seen above  $3 \times 10^{19} \text{ eV}$ . However, the resolution degrades at lower energies to about 25% at  $3 \times 10^{18} \text{ eV}$ . These Monte Carlo results were cross-checked by examination of a smaller set of stereo events where the geometry is more precisely known. Comparing the energies reconstructed using monocular and stereo geometries, we obtained resolutions similar to those seen in simulation.

The simulation is also used to calculate the detector aperture. Simulated events were subjected to the same reconstruction and cuts applied to the data. To verify the reliability of this calculation, we compared, at different energies, the zenith angle ( $\theta$ ) and impact parameter ( $R_p$ ) distributions, which define the detector aperture. The Monte Carlo predictions for these are sensitive to details of the simulation, including the detector triggering, optical ray-tracing, signal/noise, and the atmospheric modeling. We saw very good agreement between data and simulation. For example, we show the comparison of  $R_p$  distributions at three energies in Figure 1.

The analysis of HiRes-II monocular data was similar to that for HiRes-I. The data sample was collected during 142 hours of good weather between Dec. 1999 and May 2000. This period represents the first stable running of the HiRes-II detector. At the end of this period, a considerable change was made in the trigger, so that subsequently collected data will be analyzed separately. With the greater elevation coverage at HiRes-II, it was feasible to reconstruct the shower geometry from timing alone (the PCF is unnecessary), therefore we were able to loosen some cuts for the HiRes-II fits. At this stage 104,048 downward-going events remained.

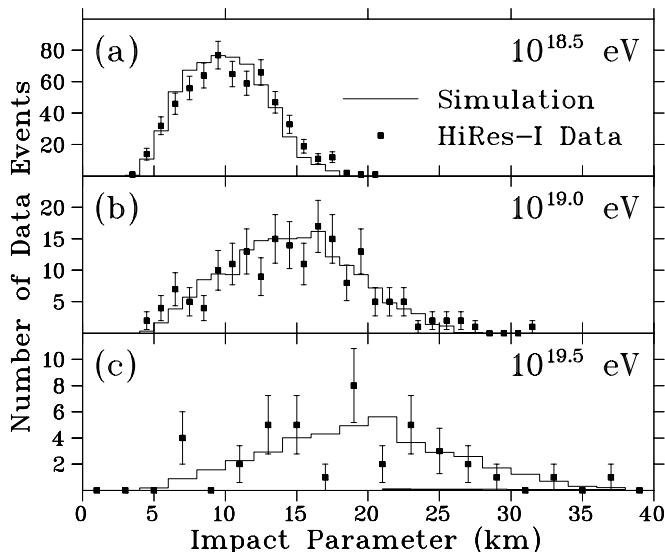


FIG. 1: Comparison of HiRes-I simulated (histogram) and observed (points)  $R_p$  distributions at (a)  $10^{18.5}$ , (b)  $10^{19.0}$ , and (c)  $10^{19.5}$  eV. The Monte Carlo distributions are normalized to the number of data events.

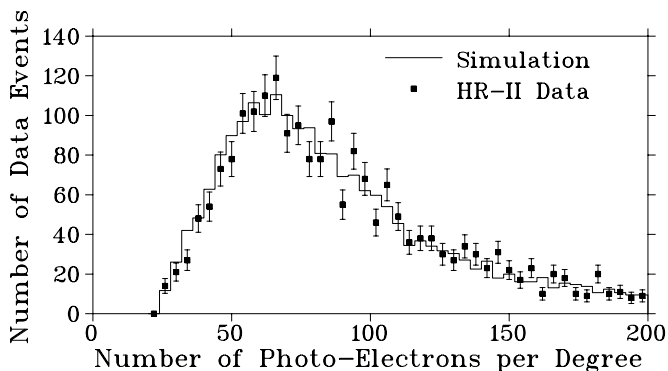


FIG. 2: A comparison of the number of photo-electrons per degree of track seen in HiRes-II monocular events (data points) and in simulation (histogram).

With the geometry of the shower known, we fit the measured shower profile to the Gaisser-Hillas parameterization [9]. The events were required to have a good fit to the Gaisser-Hillas function, to have a track length greater than  $10^\circ$  for upper ring or multi-mirror events, a track length greater than  $7^\circ$  for lower ring events, an angular speed less than  $11^\circ/\mu\text{s}$  (the larger cut for HiRes-II reflects its extended elevation coverage), a zenith angle less than  $60^\circ$ , and a shower maximum visible in our detector. There was also a cut on the size of the Čerenkov light subtraction at  $< 60\%$  of signal. Again, the same selections and cuts were applied to both simulated and real events. There were 781 events left after these cuts. These simulations also gave excellent reproduction of the data, as seen, for example, in the comparison of the number of photo-electrons per degree of track in Fig. 2.

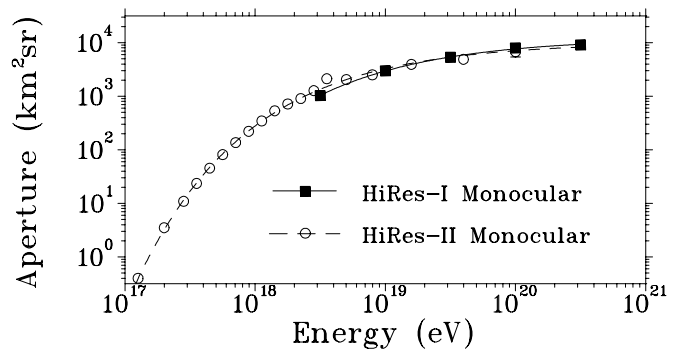


FIG. 3: Calculated HiRes monocular Reconstruction aperture in the energy range  $10^{17} - 3 \times 10^{20}$  eV. The HiRes-I and II apertures are shown by the squares and circles, respectively.

For both HiRes-I and HiRes-II events, the photoelectron count was converted to a shower size at each atmospheric depth, using the known geometry of the shower, and corrected for atmospheric attenuation. We integrated the resulting function over  $x$  and then multiplied by the average energy loss per particle to give the visible shower energy. A correction for energy carried off by non-observable particles to give the total shower energy ( $\sim 10\%$ ) [11] was then applied.

The monocular reconstruction apertures are shown in Fig. 3; both HiRes-I and HiRes-II approach  $10^4$  km<sup>2</sup> steradian above  $10^{20}$  eV. We restrict our result for HiRes-I to energies  $> 3 \times 10^{18}$  eV; below this energy the PCF technique is unstable. Due to longer tracks and additional timing information, the RMS energy resolution for HiRes-II remains better than 30% down to  $10^{17}$  eV. However, the HiRes-II data sample becomes statistically depleted above  $10^{19}$  eV.

We calculated the cosmic ray flux for HiRes-I above  $3 \times 10^{18}$  eV, and for HiRes-II above  $2 \times 10^{17}$  eV. This combined spectrum is shown in Fig. 4, where the flux  $J(E)$  has been multiplied by  $E^3$ . The most recent spectrum from the AGASA experiment[14] is also shown. The error bars represent the 68% confidence interval for the Poisson fluctuations in the number of events. The HiRes-I flux is the result of two independent analyses [15, 16].

The largest systematic uncertainties are the absolute calibration of the photo-tubes ( $\pm 10\%$ ) [6], the fluorescence yield ( $\pm 10\%$ ) [3], the correction for unobserved energy in the shower ( $\pm 5\%$ ) [11, 17], and the modeling of the atmosphere [7]. To test the sensitivity of the flux measurement to atmospheric uncertainties, we generated new Monte Carlo samples with  $\tau_A$  altered by  $\pm 1$  RMS value, from 0.04 to 0.06 and 0.02, respectively. The data and new simulated samples were then reconstructed with the altered atmospheric parameters. Averaged over energy, the flux  $J(E)$  changed symmetrically by a corresponding  $(\pm 15 \pm 5)\%$ . The systematic uncertainty in the mean  $\tau_A$  value is smaller than the RMS deviation of 0.02. This  $\pm 15\%$  change therefore represents a conser-

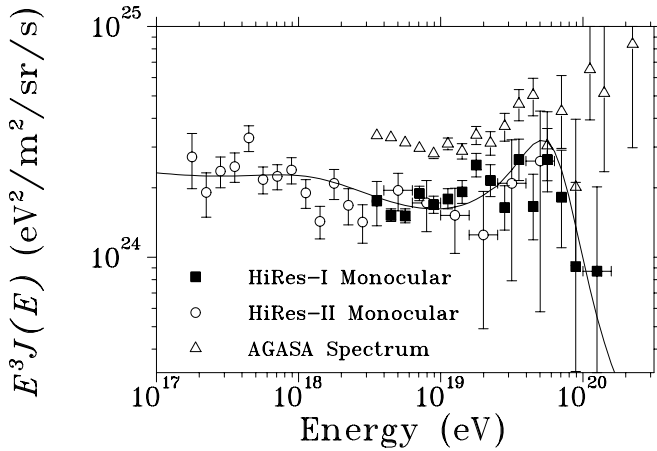


FIG. 4: Combined HiRes monocular energy spectrum. The squares and circles represent the cosmic ray differential flux  $J(E)$ , multiplied by  $E^3$ , measured by HiRes-I and HiRes-II, respectively. The line is a fit to the data of a model, described in the text, of galactic and extra-galactic cosmic ray sources. The AGASA spectrum shown is taken from their web site[14].

vative over-estimate of the one standard deviation systematic uncertainty from atmospheric effects. If we add in quadrature this uncertainty to the others mentioned above, we find a net systematic uncertainty in  $J(E)$  of 21%. This uncertainty is common to the fluxes for HiRes-I and II. There is an additional relative calibration uncertainty between the two sites of less than 10%.

Our spectrum contains two events which reconstruct with energies greater than  $10^{20}$  eV, measured at  $1.0 \times$  and  $1.5 \times 10^{20}$  eV. The fitted geometries were insensitive to variations in aerosol parameters. Assuming a purely molecular atmosphere ( $\tau_A = 0.0$ ), we obtain a lower energy limits of  $0.9 \times$  and  $1.2 \times 10^{20}$  eV.

In the energy range where both detectors' data have good statistical power, the results agree with each other very well. The data are consistent with previous experiments which observed the second knee at about  $7 \times 10^{17}$  eV, and the ankle at about  $4 \times 10^{18}$  eV [18].

The AGASA results shown in Fig. 4 suggest that the spectrum rises like a power law above the "ankle", and does not turn over at the pion-production threshold. To test whether our data are consistent with this interpretation we first fit our data from the ankle to the pion production threshold (from  $\log E$  of 18.7 to 19.8) to a power law. This fit yields an index of  $-2.81 \pm 0.06$ . Our three data points above 19.8 are not consistent with that power law continuing (26.2 events are predicted where only 10 are observed, a Poisson probability of  $2.8 \times 10^{-4}$ ).

Our data are consistent with the GZK cutoff. As an example of what one would expect, we have fit the data to a model that consists of galactic and extra-galactic sources [19], that includes the GZK cutoff. We use the extra-galactic source model of Berezhinsky *et al.* [20], where

we assume (a) protons to come from sources distributed uniformly across the universe with a maximum at-source energy of  $10^{21}$  eV, and (b) a galactic spectrum consistent with observations that the composition changes from heavy to light near  $10^{18}$  eV. The  $\chi^2$  of this fit is 48.5 for 37 degrees of freedom, and the fit is shown in Fig. 4. Details can be found in [21]. In this model the fall-off above  $\log E$  of 19.8 is due to crossing the pion production threshold, and the second knee comes from  $e^+e^-$  pair production pile-up.

This work is supported by US NSF grants PHY-9321949 PHY-9974537, PHY-9904048, PHY-0071069, PHY-0140688, by the DOE grant FG03-92ER40732, and by the Australian Research Council. We gratefully acknowledge the contributions from the technical staffs of our home institutions and the Utah Center for High Performance Computing. The cooperation of Colonels E. Fischer and G. Harter, the US Army, and the Dugway Proving Ground staff is greatly appreciated.

- 
- [1] K. Greisen, Phys. Rev. Lett. **16**, 748, (1966).
  - [2] G.T. Zatsepin and V.A. K'uzmin, Pis'ma Zh. Eksp. Teor. Fiz. **4**, 114 (1966) [JETP Lett. **4**, 78 (1966)].
  - [3] A.N. Bunner, Ph.D. Thesis (Cornell University) (1967), F. Kakimoto *et al.*, NIM **A372**, 527 (1996).
  - [4] T. Abu-Zayyad *et al.*, Proc. 26th ICRC (Salt Lake City), **5**, 349, (1999).
  - [5] J. Boyer *et al.*, NIM **A482**, 457 (2002).
  - [6] T. Abu-Zayyad *et al.*, to be submitted to NIM.
  - [7] T. Abu-Zayyad *et al.*, in preparation, and <http://www.cosmic-ray.org/atmos/>.
  - [8] R.M. Baltrusaitis *et al.*, NIM **A240**, 410 (1985).
  - [9] T. Gaisser and A.M. Hillas, Proc. 15th ICRC (Plovdiv), **8**, 353, (1977).
  - [10] T. Abu-Zayyad *et al.*, Astropart. Phys. **16**, 1, (2001).
  - [11] C. Song, Z. Cao *et al.*, Astropart. Phys. **14**, 7, (2000).
  - [12] D. Heck, J. Knapp, J.N. Capdevielle, G. Schatz and T. Thouw "CORSIKA : A Monte Carlo Code to Simulate Extensive Air Showers", Report FZKA 6019 (1998), Forschungszentrum Karlsruhe.
  - [13] N.N. Kalmykov, S.S. Ostapchenko and A.I. Pavlov, Nucl. Phys. B (Proc. Suppl.) **52B**, 17, (1997).
  - [14] The AGASA Spectrum taken from <http://www.akeno.icrr.u-tokyo.ac.jp/AGASA/>
  - [15] T. Abu-Zayyad, Ph.D Thesis, University of Utah (2000).
  - [16] X. Zhang, Ph.D Thesis, Columbia University (2001).
  - [17] J. Linsley, Proc. 18th ICRC (Bangalore), **12**, 135, (1983).
  - [18] D.J. Bird *et al.*, Phys. Rev. Lett. **71**, 3401, (1993).
  - [19] E. Waxman, Astrophys.J.Lett. 452, L1 (1995), J.N. Bahcall & E. Waxman, Phys.Lett. **B556** (2003) 1-6.
  - [20] V. Berezhinsky, A.Z. Gazizov, and S.I. Grigorjeva, hep-ph/0204357, Scully and Stecker 2002, Astropart. Phys. **16**, 271
  - [21] T. Abu-Zayyad *et al.*, astro-ph/0208301, submitted to Astropart. Phys.